Polyamidoamine (Yet Not PAMAM) Dendrimers as Bioinspired Materials for Drug Delivery: Structure−Activity Relationships by Molecular Simulations†

Lorenzo Metullio,‡ Marco Ferrone,‡ Alessandro Coslanich,‡ Sabine Fuchs,§ Maurizio Fermeglia,‡ Maria Silvia Paneni,‡ and Sabrina Pricl*,‡

Computer-aided Systems Laboratory, Department of Chemical Engineering, University of Trieste, Piazzale Europa 1, I-34127 Trieste, Italy, and Freie Universität Berlin, Insitut für Chemie/Organische Chemie, Takustrasse 3, D-14195 Berlin, Germany

Received March 9, 2004; Revised Manuscript Received May 11, 2004

In this paper, we report the results obtained from a comprehensive characterization of newly synthesized dendrimeric molecules in a solvated environment, by computer-aided simulations. The evidences allowed us to formulate some structure−activity relationships (SARs) between the experimentally verified cytotoxicity/noncytotoxicity of these compounds and some molecular features such as, for instance, radius of gyration, molecular shape, and dimensions. In particular, all noncytotoxic dendrimers were characterized by a more dense and globular shape and by a smoother surface pattern, as quantified by their fractal dimension *D*.

Introduction

Dendritic architecture is undoubtedly one of the most pervasive topologies observed universally throughout biological systems. These patterns are found at virtually all dimensional length scales (a term that refers to the best use of space). They appear in many diverse prototypes, including those that can be measured in meters (e.g., tree branching and roots), in circulatory topology in the human anatomy (e.g., lungs, kidney, liver, spleen) that are found in nm and cm, or in cerebral neurons in μm. On analysis of these ubiquitous dendritic patterns it is evident that these highly branched architectures offer unique interfacial and functional performance advantages at all levels in the biologic hierarchy.

The term dendrimers derives from the ancient Greek words *dendra* = tree and *meros* = part and describes graphically the structure of this relatively new class of macromolecules which have highly branched, three-dimensional features that resemble the architecture of a tree.[1] A typical dendrimer generation consists of three main structural components: a multifunctional central core (yellow), branched units (green), and surface groups (red; see Figure 1).

By definition or construction, these three components are interdependent and reflect a unique molecular genealogy. As we progress from the initiator core to an advanced dendrimer stage (or generation), this molecular genealogy manifest itself in a variety of ways. Thus, as a molecular-level parallelism with higher organism, beginning with the core, molecular details are sequentially transcribed and stored to produce interior and ultimately exterior features which are characteristic of that dendrimer family.[2]

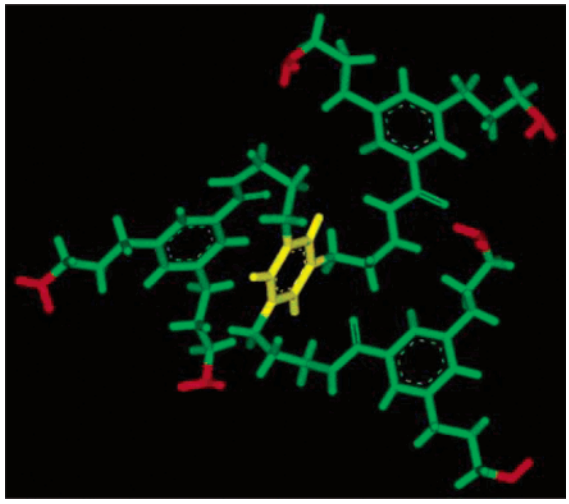

Figure 1. Major architectural components of a dendrimer molecule: initiator core (yellow), branched units (green), and surface groups (red).

The growing body of clinical data arising from the development of polymer therapeutics suggests that polymer−protein and polymer−drug conjugates constitute an important new class of anticancer agents.[3−5] This has aroused considerable interest in the design of second generation polymer-based anticancer treatments, and also in the potential use of polymer therapeutics for management of other diseases. Traditionally, a polymer−drug conjugate comprise a linear, hydrophilic polymer backbone covalently bound to a potent antitumor drug via a biodegradable spacer. However, with respect to their linear counterpart, dendrimeric polymers (alternatively called arborols or cascade molecules) offer particular advantages as (a) they possess narrow polydispersity, (b) they display the possibility to tailor-make their

† Part of these results were presented at the 2003 AIChE annual meeting, November 16−21 2003, San Francisco, CA, paper #472b, session 472: Bioinspired and Biomimetic Materials I.

* To whom correspondence should be addressed. Phone: +39-040-5583750. Fax: +39-040-569823. E-mail: sabrinap@dicamp.units.it.

‡ University of Trieste.

§ Freie Universität, Berlin.

10.1021/bm049858x CCC: $27.50
Published on Web 06/19/2004

surface chemistry, and (c) the reduced structural density in the intramolecular core is amenable to host−guest entrapment with opportunities for subsequent release of active principles which are either water insoluble (or sparing soluble) or characterized by a high toxicity. A detailed summary of dendrimer applications in medicine is outside the aim of this work; as a glimpse, however, these dendritic molecules hold promise as novel drug carriers, gene delivery systems, imaging agents, in tissue targeting applications and controlled drug release.[6−11]

For a polymeric carrier to be suitable for in vivo applications, it is essential that the carrier is nontoxic, nonimmunogenic, and preferably biodegradable. Further, it must display an inherent body distribution that will allow appropriate tissue targeting. Under these perspectives, the polyamidoamine (PAMAM) family is actually widely used as transfection agents for DNA into living cells,[12−16] whereas others are employed as contrast agents for magnetic resonance imaging (MRI)[17,18] and in boron neutron capture therapy (BNCT)[19−22] in cancer treatment. On the spur of these applications, some studies of the behavior in cell culture, as well as in living organism, of this dendrimeric family, both pristine and modified, have been carried out.[23,24] As a major finding, the authors discovered that cationic dendrimers were cytotoxic, with a degree of toxicity depending on dendrimer type, cell type, and generation. They also caused hemolysis and changes in erythrocyte morphology. In contrast, anionic dendrimer derivatives (e.g., surface-modified with −COOH moieties) were neither hemolytic nor cytotoxic.

Despite such advances, it appears clear that a substantial understanding of the inherent structure/toxicity relationship of dendrimers is still at large, given also the fact that each dendrimer type, and each generation within each type, could have its own behavior and mechanism of toxicity in biological systems. Accordingly, it is necessary to explore in grater detail the influence of different surface functionalization of otherwise identical dendrimers on their in vitro and in vivo behavior, as this constitute a prerequisite for considering these branched macromolecules as drug delivery systems, e.g., as novel carriers for anticancer drugs.

Quite recently, Fuchs et al. have reported in the literature the synthesis, in vitro cytotoxicity, and intracellular localization of four new sets of first and second generation polyamidoamine (yet not PAMAM) dendrimers, which differ only in surface motifs.[25] Accordingly, they used (a) quaternized amines (set A dendrimers), (b) L-phenylalanine, L-methionine, and L-aspartic acid (set B dendrimers), (c) diaminopropionic acid (set C dendrimers), (d) the 5-dimethylamino-naphthalene-1-sulfonyl chloride (dansyl) motif (set D dendrimers), and (e) a mixture of the above listed decorating groups (set E; see Chart 1). Some of the modified dendrimers carry chelating ligands for PtII (e.g., L-methionine, diaminopropionic acid), and could thus be potentially used for binding cisplatin-like complexes.[26,27] Further, all dendrimer sets A−C were used to perform a systematic exploration of the influence of surface decoration on the dendrimer cytotoxicity; the dansylated molecules of set D were considered to study cellular uptake and intracellular distribution using confocal fluorescence microscopy. As a major finding of this work, Fuchs et al.[25] proved that positive charges on a dendrimer surface, as well exemplified by dendrimer set C, cannot be routinely associated to cell toxicity, as one could have been inclined to conclude from literature results.[24,28−30]

Thus, although dendrimer surface functionalization grossly influenced dendrimer cytotoxicity, a coherent structure/toxicity correlation could not be established (see Table 1). Therefore, we decided to attempt a structure/activity (SAR) relationship for all these dendrimer sets by means of molecular modeling. To this purpose, we decided to apply detailed, atomistic molecular dynamics simulation techniques to investigate whether some correlations could be established between peculiar dendrimeric features, such as molecular shape and dimension, radius of gyration, density and fractal dimension, and the corresponding experimentally verified cytotoxicity/noncytotoxicity of these molecules.

Computational Details

All calculations were carried out on a cluster of 16 Silicon Graphics Octane R12K, running Irix 6.5.18 operating system. The all-atom force field (FF) parameters by Cornell et al.[31] (in parm94.dat file of the AMBER 6.0 code package[32,33]) was applied in all simulations. The model structures of all dendrimer sets A−E (see Chart 1) were generated using the Biopolymer module of InsightII.[34] Geometry refinement was carried out using the SANDER module of AMBER via a combined steepest descent − conjugate gradient algorithm, using as a convergence criterion for the energy gradient the root-mean-square of the Cartesian elements of the gradient equal to 10^{-3} kcal/(mol Å). The conformational search was carried out using a well-validated, combined molecular mechanics/molecular dynamics simulated annealing (MDSA) protocol.[35−39] Accordingly, the relaxed structures were subjected to five repeated temperature cycles (from 300 to 1000 K and back) using constant volume/constant temperature (NVT) MD conditions. At the end of each annealing cycle, the structures were again energy minimized to converge below 10^{-3} kcal/(mol Å), and only the structures corresponding to the minimum energy were used for further modeling. To let the dendrimers relax in an aqueous environment, each molecule was immersed in a cubic box of TIP3P-water molecules,[40] extended at least 10 Å in each direction from the solute. According to Fuchs et al.,[25] all dendrimers were ionized at the experimental pH. Therefore, each dendrimer was neutralized adding a suitable number of counterions (Na^+ and Cl^-) in the positions of largest electrostatic potential, as determined by the module CION of the AMBER 6.0 platform. The periodic boundary conditions with constant pressure of 1 atm were applied, and the particle mesh Ewald (PME) method[41] was used to treat the long-range electrostatics. Unfavorable interactions within the structures were relieved with steepest descent followed by conjugate gradient energy minimization until the RMS of the elements in the gradient vector was less than 10^{-3} kcal/(mol Å). Each system was gradually heated to 300 K in three intervals, allowing a 5 ps interval per each 100 K and then equilibrated for 250 ps at 300 K, followed by 2.5 ns of data

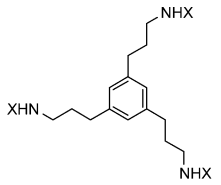

4

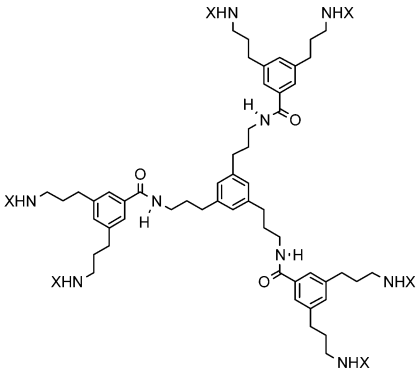

8

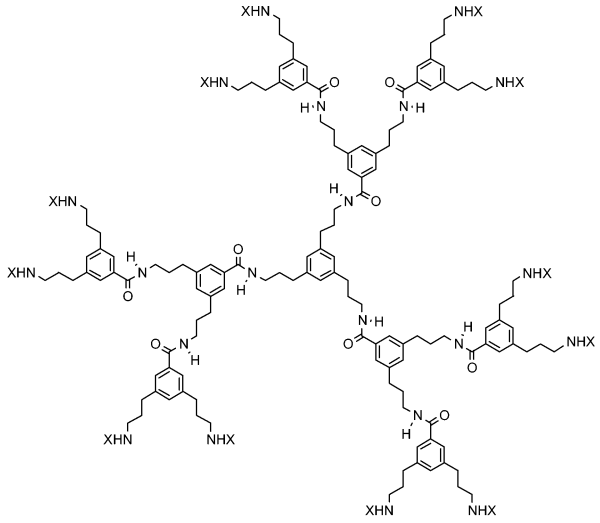

10

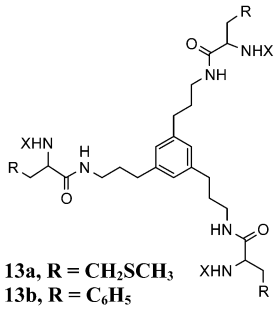

13a, R = CH_2SCH_3
13b, R = C_6H_5
13c, R = COOH

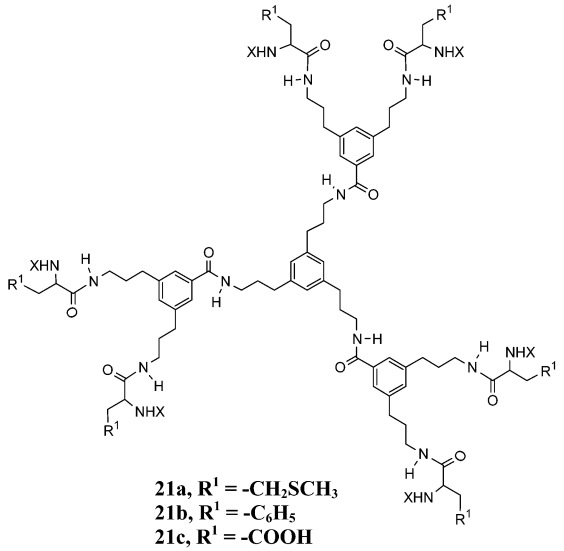

21a, R^1 = -CH_2SCH_3
21b, R^1 = -C_6H_5
21c, R^1 = -COOH

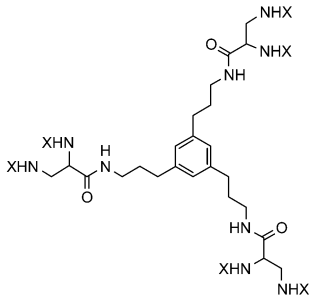

16

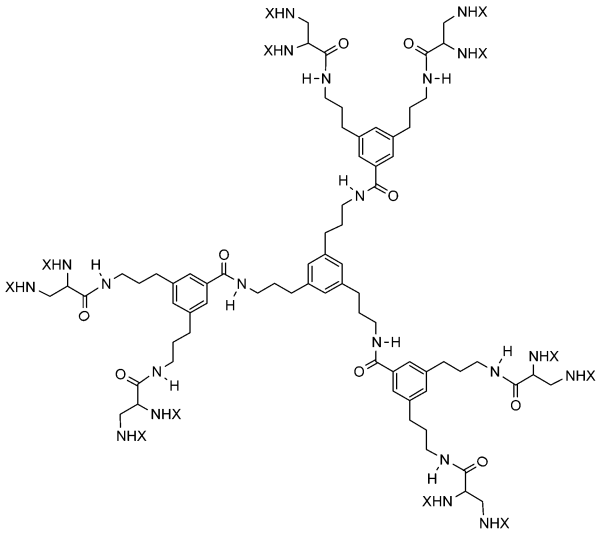

25

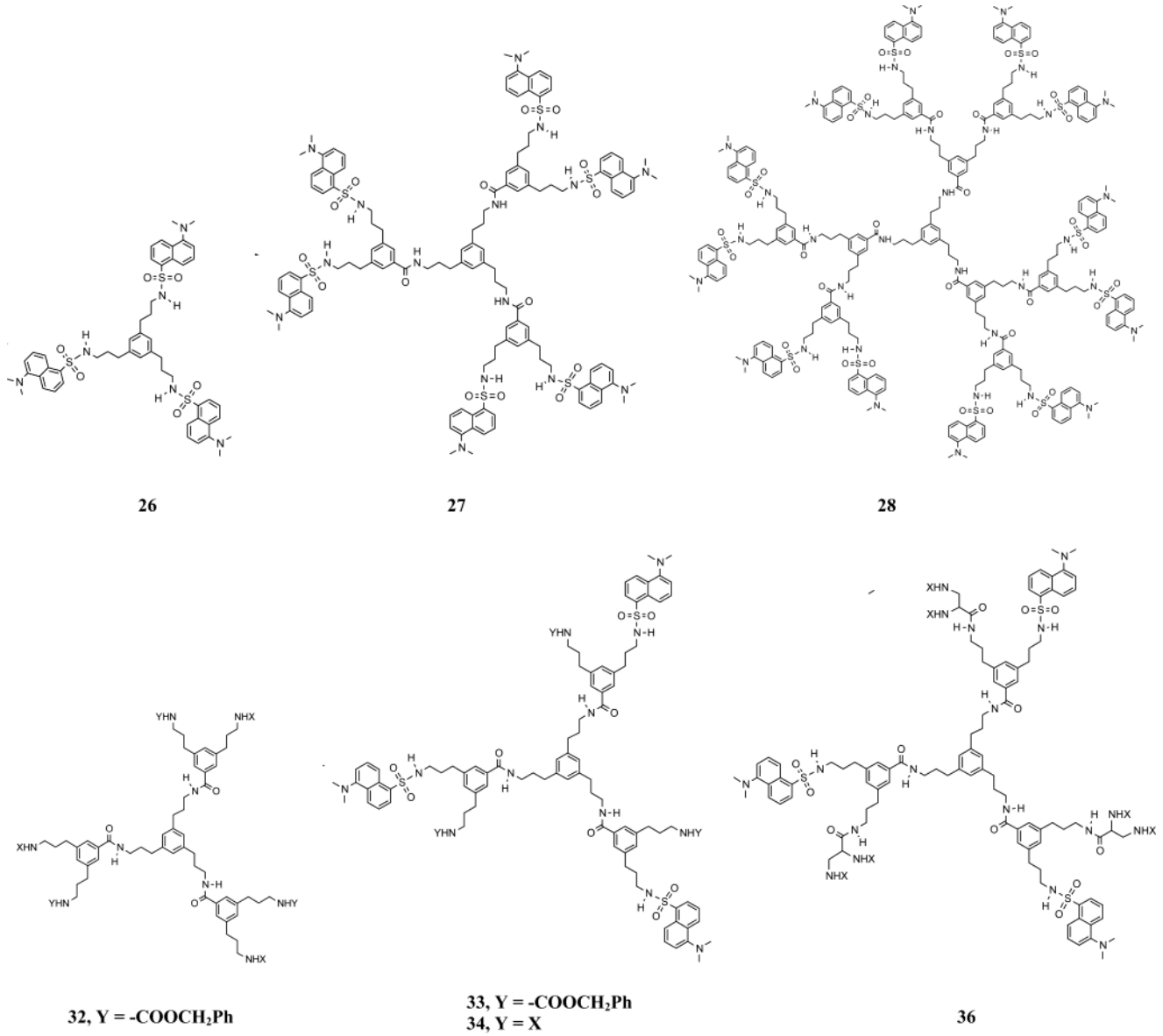

Chart 1. In All Structures, X = H·HCl; Dendrimer Set A: **4**, **8**, **10**; Dendrimer Set B: **13**, **21**; Dendrimer Set C: **16**, **25**; Dendrimer Set D: **26**, **27**, **28**; Dendrimer Set E: **32**, **33**, **34**, **36**.

Table 1. Experimental Cytotoxicity of All Dendrimer Sets (Data from ref 25)[a]

set A		set B		set C		set D		set E	
4	NT	**13c**	NT	**16**	NT	**26**	NT	**32**	HT
8	T	**21c**	NT	**25**	NT	**27**	NT	**33**	HT
10	HT	**13a**	NT			**28**	NT	**34**	HT
		21a	MT					**36**	HT
		13b	T						
		21b	T						

[a] NT = non cytotoxic; MT = moderately cytotoxic; T = cytotoxic; HT = highly cytotoxic.

collection runs. A Verlet leapfrog[42] integration time step of 2 fs has been used with constant temperature, with the temperature being maintained at a constant value by the Berendsen coupling algorithm,[43] with separate solute−solvent and solvent−solvent coupling. A total of 2500 snapshots were saved during the data collection period, one snapshot per each 1 ps of MD simulation. Finally, to limit the effect due to a peculiar distribution of the water molecules within the cubic box, 10 independent structures for each solvated dendrimeric molecule considered in this study were generated, according to the procedure described above. The properties described below are then to be considered as ensemble averaged from the appropriate set of 10 structures. The 10 simulations for the largest system considered (i.e., dendrimer **28** in a water cubic box of 62 Å × H 62 Å × H 62 Å) required approximately 42 days of CPU time.

The calculation of molecular surfaces, the solvent accessible surfaces, and the associated volumes was performed using both the so-called Connolly dot surfaces algorithm[43−45] and the MSMS[46] program. Each measure of surface/volume is averaged over 250 equilibrated structures extracted from the corresponding MD trajectory.

Results and Discussion

Figure 2 shows an example of equilibrated structures of some dendrimers belonging to sets A and C, obtained as a result of the first structural investigations performed with MD simulations.

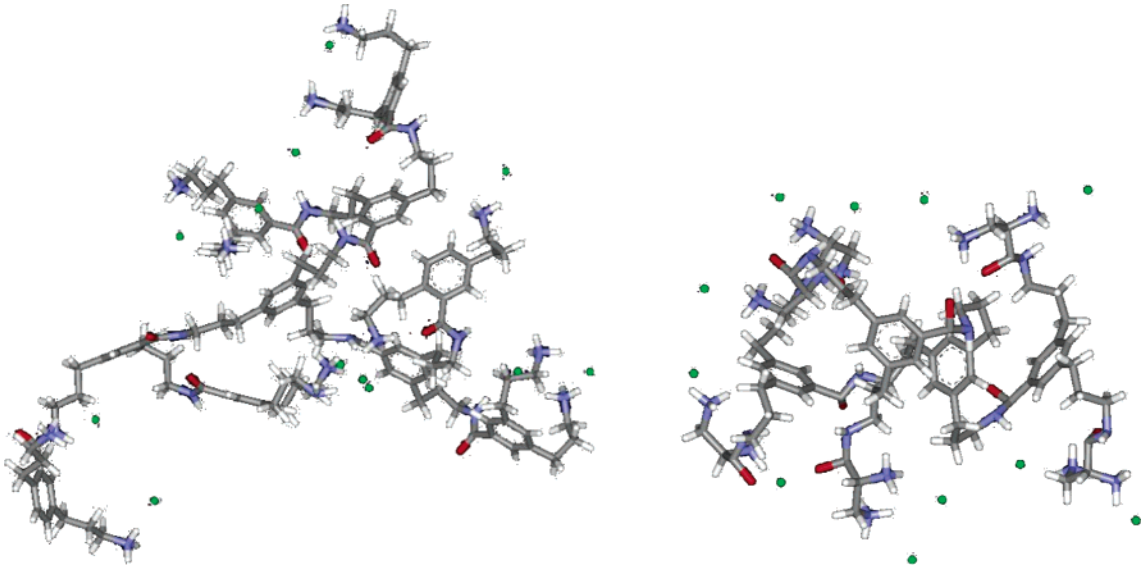

Figure 2. MD equilibrated structures of dendrimer **10** (set A, left) and dendrimer **25** (set C, right). Water molecules have been omitted for clarity.

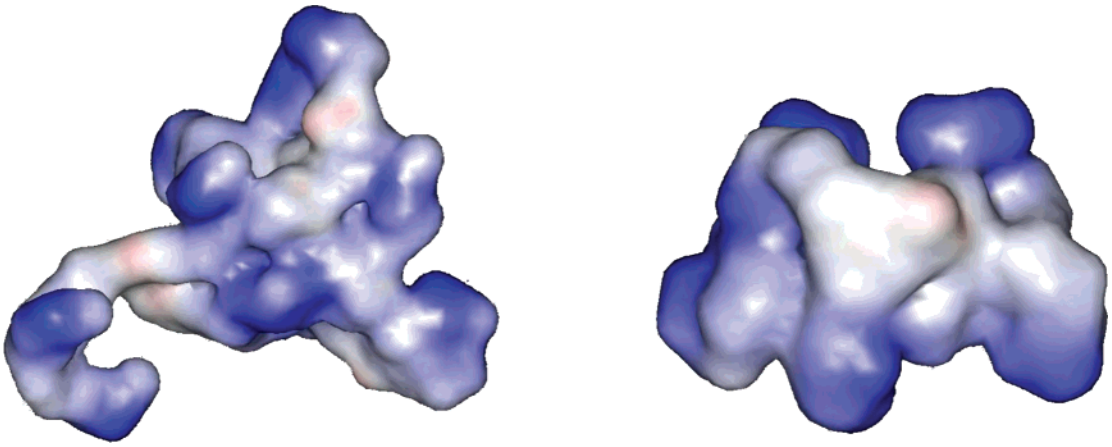

Figure 3. van der Waals molecular surface of dendrimer **10** (set A, left) and dendrimer **25 (**set C, right).

From a quick inspection of this figure, we can observe how dendrimers endowed with cytotoxicity possess a more open structure, reminiscent of a starfish, whereas those that are noncytotoxic are characterized, already at early generations, by an overall spherical shape (see Figure 2). This can be better apprised by considering Figure 3, in which we report, as an example, the graphical representation of the van der Waals molecular surface of the dendrimers **10** and **25**, respectively.

This pictorial evidence can be quantified[1] by the aspect ratio of the largest to the smallest principal moment of inertia (I_z/I_x) of all dendrimer sets reported in the first column of Table 2. Indeed, all noncytotoxic dendrimers are characterized by I_z/I_x values all close to one, indicating a spheroidal form, whereas the cytotoxic molecules have much higher values, indicating a somewhat amorphous shape.

As can also be inferred from Figure 3, the cytotoxic dendrimers have a great deal of internal surface area and solvent-filled volume, whereas the noncytotoxic molecules have very little. A quantitative comparison can be made by using the concept of solvent accessible surface (SAS).[47] The SAS is obtained by "rolling" a sphere of radius R_p (the probe radius) around the van der Waals surface of the molecule, where represents the effective radius of the solvent (e.g., $R_p = 1.4$ Å for a water molecule). The SAS is then composed of the locus of the probe−sphere midpoints.[43−46] Considering for example the surface of an ideal, spherical molecule containing no internal voids, its surface area can be defined as follows:

$$A_{SAS} = 4\pi(R + R_p)^2 \qquad (1)$$

where R is the radius of the spherical molecule and R_p is the radius of the probe. Accordingly, for spherical macromolecules a plot of $\sqrt{A_{SAS}}$ vs R_p would be linear, with a slope of $2\sqrt{\pi}$ and intercept proportional to the radius R. Obviously, none of the dendrimers considered are ideally spheroidal, but they can be treated, at least to a first approximation and for the purpose of the analysis, as such.[1] As an example, Figure 4 contains the plots of $\sqrt{A_{SAS}}$ as a function of the probe radius R_p for dendrimer **10** (set A) and dendrimer **25** (set C), respectively. Indeed, for large values of R_p, A_{SAS} becomes independent of R_p, as expected; nevertheless, for small probe radii, a deviation from linearity is observed, owing to the extra surface area associated with the interior regions of the molecules. A linear regression analysis of these data indicates both the amount of any internal surface area

Table 2. Aspect Ratio of the Largest to the Smallest Principal Moment of Inertia (I_z/I_x), Fraction of Internal Surface Area A_{int}, Fraction of Internal Volume V_{int}, and Dimensions of the Dendrimers $d_{A_{SAS}}$, $d_{V_{SAS}}$ and Maximum Diameter d_{max} for All Dendrimer Series[a]

	I_z/I_x (−)	A_{int} (%)	V_{int} (%)	$d_{A_{SAS}}$ (Å)	$d_{V_{SAS}}$ (Å)	d_{max} (Å)
set A						
4				10.6	10.6	11.0 ± 0.6
8	*2.85*	*29*	*44*	*17.6*	*18.1*	*18.2 ± 0.8*
10	*2.89*	*57*	*65*	*24.4*	*24.2*	*25.5 ± 1.1*
set B						
13c	1.53	2.1	8	15.0	14.9	15.0 ± 0.5
21c	1.17	5.3	12	25.1	25.0	25.5 ± 1.7
13a	1.57	4.2	12	13.5	13.6	13.6 ± 1.6
21a	*2.24*	*15*	*33*	*26.2*	*25.6*	*26.3 ± 18*
13b	*2.43*	*27*	*37*	*15.7*	*15.9*	*16.1 ± 1.3*
21b	*2.60*	*47*	*66*	*25.8*	*25.9*	*26.3 ± 1.6*
set C						
16	1.49	3.0	10	15.3	15.0	15.6 ± 0.4
25	1.51	4.9	14	20.0	19.7	20.0 ± 0.9
set D						
26	1.36	5.8	12	12.6	12.7	13.5 ± 1.7
27	1.24	11	16	15.5	14.8	15.6 ± 1.8
28	1.21	14	19	35.0	34.9	35.2 ± 1.3
set E						
32	*3.38*	*50*	*78*	*24.6*	*24.1*	*24.7 ± 0.9*
33	*2.95*	*58*	*77*	*26.1*	*26.0*	*26.6 ± 1.8*
34	*2.52*	*69*	*86*	*25.8*	*26.2*	*26.4 ± 1.9*
36	*2.61*	*66*	*81*	*26.2*	*25.9*	*26.2 ± 1.7*

[a] Values in italics refer to cytotoxic molecules.

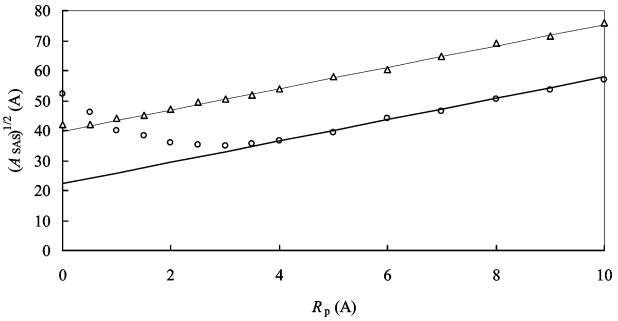

Figure 4. Plots of $\sqrt{A_{SAS}}$ as a function of the probe radius R_p for dendrimer **10** (set A, ○) and **25** (set C, △). Lines: linear regression fitting (see text).

(A_{int}) and the size of the dendrimers ($d_{A_{SAS}}$). For the cytotoxic dendrimer **10**, the fraction of internal surface is quite consistent, being equal to 57%. In contrast, for the noncytotoxic dendrimer **25**, the internal surface area peaks at 4.9%.

A measure of the volume associated with the internal cavities of the dendrimers, V_{int}, can be achieved analyzing the behavior of the volume contained within the calculated A_{SAS}s, V_{SAS}, again as a function of the probe radius R_p. Reconsidering the example of the ideally spherical molecule, devoid of internal cavities, the volume contained within the A_{SAS} of the sphere is given by the following relationship:

$$V_{SAS} = \frac{4}{3}\pi(R + R_p)^3 \qquad (2)$$

Accordingly, a plot of $(V_{SAS})^{1/3}$ vs R_p should be linear, with a slope of $(4/3\pi)^{1/3}$ and an intercept proportional to the radius R. Indeed, in the case of our dendrimers, eq 2 is satisfied for large probe radii (data not shown), but there is a deficit of volume for small probes, owing to the presence of the internal cavities and channels. Nonetheless, although the fraction of internal volume is quite limited for all noncytotoxic dendrimers (from 8% of dendrimer **13c** to 19% of dendrimers **28**), the opposite trend can be observed in the case of cytotoxic molecules, where V_{int} ranges from 33% of dendrimer **21a** to 86% of dendrimer **34**. Table 2 gathers the values of A_{int}, V_{int}, $d_{A_{SAS}}$ and $d_{V_{SAS}}$ for all dendrimers analyzed in this work. As we can see from this table, low fractions of internal surface areas and internal volumes characterize all noncytotoxic dendrimers, whereas the cytotoxic series present higher values of A_{int} and are characterized by the presence of crevices and pits between the branches, allowing for high values of V_{int}. Thus, the overall dramatic structure-based difference between the cytotoxic and noncytotoxic dendrimer series is once again quite evident.

Molecular dynamics simulations were also used to estimate d_{max}, that is the maximal end-to-end distance between terminal heteroatoms (see Table 2). This quantity was determined periodically and averaged over the entire set of trajectories, and its value should in principle provide an upper bound, since it emphasizes any dangling arms protruding out of the dendrimer. Generally speaking, there is a very good agreement between all values calculated from different evidences, and the d_{max} indeed provide an upper bracket to the other calculated diameters.

One of the most important problems in structural biology is the origin of specificity and recognition in molecular interactions. An essential step in this process is complementary contact between approaching molecular surfaces. Surface representation of macromolecules such as, in our specific case, dendrimers, have provided a powerful approach for characterizing the structure, folding, interactions, and properties of these molecules. A fundamental features of surfaces that has not been characterized by these representations, however, is the texture (or roughness) of polymer surfaces, and its role in molecular interactions has not been defined. The degree of irregularity of a surface may be described[48] by means of a fractal dimension D. Fractal geometry is a mathematical tool for dealing with complex systems that have no characteristic length scales. Scale-invariant systems are usually characterized by noninteger (i.e., fractal) dimensions, and hence, the objective of any fractal analysis is to find a relationship of some kind of power-law

$$\text{physical property} \propto \text{variable}^{\text{scaling exponent}} \qquad (3)$$

where the variable and the exponent are related to the fractal dimension. This relation is obviously one that can cover a very broad range of molecular structures; however, this kind of power law requires some symmetry in these structures.

According to its definition, as a molecular surface becomes more irregular, the corresponding fractal dimension increases, starting from its lower value $D = 2$, equivalent to an entirely smooth surface. According to a known procedure,[49,37,38] the value of D may be obtained from the slope of the log(surface

Table 3. Surface Fractal Dimension D, Radius of Gyration R_g, Density ρ, and Molecular Mass for All Dendrimer Series[a]

	D (−)	R_g (Å)	ρ (g/cm^3)	MM (−)
set A				
4	2.01	4.8 ± 0.7	1.491 ± 0.003	45
8	*2.18*	*7.8 ± 0.8*	*1.437 ± 0.003*	*147*
10	*2.21*	*10.7 ± 1.0*	*1.396 ± 0.003*	*351*
set B				
13c	2.01	7.3 ± 0.9	1.612 ± 0.002	594
21c	2.05	9.9 ± 0.9	1.655 ± 0.003	1594
13a	2.09	6.4 ± 0.8	1.661 ± 0.002	642
21a	*2.19*	*9.1 ± 1.0*	*1.520 ± 0.003*	*1690*
13b	*2.25*	*7.1 ± 0.8*	*1.432 ± 0.004*	*690*
21b	*2.29*	*11.7 ± 1.0*	*1.393 ± 0.005*	*1786*
set C				
16	2.00	6.7 ± 0.8	1.890 ± 0.004	507
25	2.03	9.1 ± 0.9	1.826 ± 0.004	1420
set D				
26	2.01	6.7 ± 0.8	1.777 ± 0.004	948
27	2.00	8.6 ± 1.0	1.790 ± 0.003	2302
28	2.01	12.7 ± 1.1	1.745 ± 0.004	5009
set E				
32	*2.25*	*8.5 ± 0.9*	*1.383 ± 0.002*	*1307*
33	*2.22*	*10.1 ± 1.1*	*1.484 ± 0.0023*	*1603*
34	*2.27*	*11.4 ± 1.1*	*1.335 ± 0.003*	*2005*
36	*2.20*	*13.9 ± 1.0*	*1.442 ± 0.001*	*1861*

[a] Values in italics refer to cytotoxic molecules.

area) against log(probe size) used by the MSMS program[46] to determine the molecular surface as follows:

$$2 - D = \frac{\mathrm{d}\log(A_{SAS})}{\mathrm{d}\log(R_p)} \quad (4)$$

in which A_{SAS} and R_p are again the molecular surface area and probe radius, respectively. Interestingly, in the case of cytotoxic dendrimers, such as dendrimer set E for instance, the value of D increases from 2.20 for **36** to 2.27 for **34**, whereas in the case of the noncytotoxic dendrimers (e.g., set C), the corresponding value of D stays flat and close to the lower limit of 2 (2.01 and 2.05 for **13c** and **21c**, respectively), even at intermediate values of R_p. Table 3 lists the calculated surface fractal dimensions for all dendrimer series, from where the analogies between cytotoxic and noncytotoxic dendrimers, in terms of fractal surface dimensions, is quite evident. It is further worthwhile noticing that the calculated surface fractal dimensions are close to those characterizing various protein and biomacromolecules, which vary, just to cite a few, between 2.05 for DNA to 2.62 for trypsin.[50]

The radius of gyration R_g is a fundamental tool for the characterization of the structural properties of dendrimers. This quantity is defined as the square root of the second invariant of the first-order tensor **S**, which accounts for the spatial distribution of the atom chains by mediating over all N molecular components. The R_g values estimated by molecular dynamics simulations for all dendrimer sets are reported in Table 3. Again, a major distinction can be observed between noncytotoxic and cytotoxic molecules: at comparable molecular mass, the former are characterized by smaller values of R_g, further indication for compact, space filling structures, whereas the latter possess a broader distribution of the mass around their center of gravity, in harmony with the larger internal volume available.

The density of each dendrimer molecule in a solvated environment, calculated from NPT MD simulations, is reported in Table 3. As expected, these data agree with all previous findings; that is, noncytotoxic dendrimers possess higher density values with respect to their cytotoxic counterparts. In particular, it is interesting to observe that dendrimers of set E, which feature the lowest density values, are also the most cytotoxic, dendrimer **34** being even cytocidal at all experimental concentration tested.[25]

Conclusions

All anionic PAMAM-based dendrimers synthesized by Fuchs et al.[25] and modeled in the present work exhibited no measurable cytotoxicity at all concentrations tested. In contrast, not all cationic dendrimers showed cytotoxicity toward MCF-7 cell cultures at concentrations between 1 and 20 μM. Further, neutral dendrimers of set D were all noncytotoxic whereas, contrarily to expectations, dendrimers of set E all prevented cell proliferation, dendrimer **34** reaching even cytocidal effects. In the case of polycations, it is generally accepted that electrostatic interactions between positive charges on the cationic macromolecule, and negatively charged sites on the cells, which are recognized as a universal characteristic of the cell membrane, induces cell membrane damage and leads to cell death.[51−53] Nevertheless, according to Choksakulnitmir,[28] the different degree of cytotoxicity induced by polycations may be due to the balancing contributions of different factors, ranging from difference in the density of positive charges, molecular size and structure could be invoked to explain the experimental results. Under this perspective, the detailed molecular modeling procedure adopted in this work, based on our previous experience on this specific subject,[36,38,49,54] allowed us to formulate, for the first time, a SAR between the in vitro data and some peculiar molecular features of dendrimers, such as radius of gyration, density, shape, and fractal dimension. All data from different calculations lead to the definition of a common trend, in harmony with literature speculations: the noncytotoxic molecules considered were all characterized by a more globular, compact shape, with spare internal surface area and volume, a higher density, and a smoother surface pattern, as quantified by the values of their surface fractal dimension D. Undoubtedly, more data are needed to further support these preliminary results, which are currently underway in our laboratories.

Acknowledgment. We thank the Italian Ministry for University and Research for financial support (FIRB 2001 to S.P.).

References and Notes

(1) Tomalia, D. A.; Naylor, A. M., Goddard, W. A., III. *Angew. Chem., Int. Ed. Engl.* **1990**, *29*, 138.
(2) Tomalia, D. A.; Uppuluri, S.; Swanson, D. R.; Li, J. *Pure Appl. Chem.* **2000**, *72*, 2343.
(3) Duncan, R. *Anti-Cancer Drugs* **1992**, *3*, 175.

(4) Duncan, R.; Dimitrijevic, S.; Evagororou, E. G. *Stp. Pharma Sci.* **1996**, *6*, 237.
(5) Vasey, P.; Twelves, C.; Kaye, S. B.; Wilson, P.; Morrison, R.; Duncan, R.; Thomson, A.; Hilditch, T.; Murray, T.; Burtles, S.; Cassidy, J. *Clin. Cancer Res.* **1999**, *5*, 83.
(6) Liu, M.; Fréchet, J. M. *J. Pharm. Sci., Technol. Today* **1999**, *2*, 393.
(7) Esfand, R.; Tomalia, D. A. *Drug Discuss. Today* **2001**, *8*, 427.
(8) Patri, A. K.; Majoros, I. J.; Baker, J. R., Jr. *Curr. Opin. Chem. Biol.* **2002**, *6*, 466.
(9) Boas, U.; Söntjens, S. H. M.; Jensen, K. J.; Christensen, J. B.; Meijer, E. W. *Chem. Biochem.* **2002**, *3*, 433.
(10) Cloninger, M. J. *Curr. Opin. Chem. Biol.* **2002**, *6*, 742.
(11) Aulenta, F.; Hayes, W.; Rannard, S. *Eur. Polym. J.* **2003**, *39*, 1741.
(12) Haensler J.; Szoka, F. C., Jr. *Bioconjugate Chem.* **1993**, *4*, 372.
(13) Tang, M. X.; Redemann, C. T.; Szoka, F. C., Jr. *Bioconjugate Chem.* **1996**, *7*, 703.
(14) Bielinska, A. U.; Fukowska-Latallo, J. F.; Johnson, J.; Tomalia, D. A.; Baker, J., Jr. *Nucleic Acids Res.* **1996**, *24*, 2176.
(15) Fukowska-Latallo, J. F.; Bielinska, A. U.; Johnson, J.; Spindler, R.; Tomalia, D. A.; Baker, J., Jr. *Proc. Natl. Acad. Sci. U.S.A.* **1996**, *93*, 4897.
(16) Bielinska, A. U.; Chen, C.; Johnson, J.; Baker, J. R., Jr. *Bioconjugate Chem.* **1999**, *10*, 843.
(17) Wiener, E. C.; Brechbiel, M. W.; Brothers, H.; Magin, R. L.; Gansow, A.; Tomalia, D. A.; Lauterbur, P. C. *Magn. Reson. Med.* **1994**, *31*, 1.
(18) Kobayashi, H.; Kawamoto, S.; Saga, T.; Sato, N.; Ishimori, T.; Konishi, J.; Ono, K.; Togashi, K.; Brechbiel, M. W. *Bioconjugate Chem.* **2001**, *12*, 587.
(19) Nemoto, H.; Wilson, J. G.; Nakamura, H.; Yamamoto, Y. *J. Org. Chem.* **1992**, *57*, 435.
(20) Newkome, G. R.; Moorefield, C. N.; Keith, J. M.; Baker, G. R.; Escamilla, G. H. *Angew. Chem., Int. Ed. Engl.* **1994**, *33*, 666.
(21) Armspach, D.; Cattalini, M.; Constable, E. C.; Housecroft, C. E.; Philips, D. *Chem. Commun.* **1996**, 1823.
(22) Qualmann, B.; Kessel, M. M.; Musiol, H.-J.; Sierralta, W. D.; Jungblut, P. W.; Moroder, L. *Angew. Chem., Int. Ed. Engl.* **1996**, *35*, 909.
(23) Roberts, J. C.; Bhalgat, M. K.; Zera, R. T. *J. Biomed. Mater. Res.* **1996**, *30*, 53.
(24) Malik, N.; Wiwattanapatapee, R.; Klopsh, R.; Lorenz, K.; Fery, H.; Weener, J. W.; Meijer, J. W.; Paulus, W.; Duncan, R. *J. Controlled Release* **2000**, *65*, 133.
(25) Fuchs, S.; Kapp, T.; Otto, H.; Schöneberg, T.; Franke, P.; Gust, R.; Schlüter, A. D. *Chem. Eur. J.* **2004**, *10*, 1167−1192.
(26) Verstraete, S.; Heudi, O.; Cailleux, A.; Allain, P. *J. Inorg. Biochem.* **2001**, *84*, 129.
(27) Küng, A.; Strickmann, D. B.; Galanski, M.; Keppler, B. K. *J. Inorg. Biochem.* **2001**, *84*, 691.
(28) Choksakulnitmir, S.; Masuda, S.; Tokuda, H.; Takakura, Y.; Hashida, M. *J. Controlled Release* **1995**, *34*, 233.
(29) Fischer, D.; Li, Y.; Ahlemeyer, B.; Krieglstein, J.; Kissel, T. *Biomaterials* **2003**, *24*, 1121.
(30) Jevprasesphant, R.; Penny, J.; Jalal, R.; Attwood, D.; McKewon, N. B.; D'Emanuele, A. *Int. J. Pharm.* **2003**, *252*, 263.
(31) Cornell, W. D.; Cieplak, P.; Bayly, C. I.; Gould, I. R.; Merz, K. M., Jr.; Ferguson, D. M.; Spellmeyer, D. C.; Fox, T.; Caldwell, J. W.; Kollman, P. A. *J. Am. Chem. Soc.* **1995**, *117*, 5179.
(32) Case, D. A.; Pearlman, D. A.; Caldwell, J. W.; Cheatham, T. E., III.; Ross, W. S.; Simmerling, C. L.; Darden, T. A.; Merz, K. M.; Stanton, R. V.; Cheng, A. L.; Vincent, J. J.; Crowley, M.; Tsui, V.; Radmer, R. J.; Duan, Y.; Pitera, J.; Massova, I.; Seibel, G. L.; Singh, U. C.; Weiner, P. K.; Kollman, P. A. *AMBER 6*; University of California: San Francisco, 1999.
(33) Pearlman, D. A.; Case, D. A.; Caldwell, J. W.; Ross, W. S.; Cheatham, T. E., III.; DeBolt, S.; Ferguson, D.; Seibel, G. L.; Kollman, P. A. *Comput. Phys. Commun.* **1995**, *91*, 1.
(34) InsightII Program Package (2000.1); Accelrys Inc.: San Diego, CA, 2000.
(35) Felluga, F.; Fermeglia, M.; Ferrone, M.; Pitacco, G.; Pricl, S.; Valentin, E. *Tetrahedron: Asymmetry* **2002**, *13*, 475.
(36) Fermeglia, M.; Ferrone, M.; Pricl, S. *Bioorg. Med. Chem.* **2002**, *10*, 2471.
(37) Felluga, F.; Pitacco, G.; Valentin, E.; Coslanich, A.; Fermeglia, M.; Ferrone, M.; Pricl, S. *Tetrahedron: Asymmetry* **2003**, *14*, 3385.
(38) Pricl, S.; Fermeglia, M.; Ferrone, M.; Asquini, A. *Carbon* **2003**, *41*, 2269.
(39) Manfredini, S:; Solaroli, N.; Angusti, A.; Nalin, F.; Durini, E.; Vertuani, S.; Pricl, S.; Ferrone, M.; Spadari, S.; Focher, F.; Verri, A.; De Clercq, E.; Balzarini, J. *Antivir. Chem. Chemother.* **2003**, *14*, 183.
(40) Jorgensen, W. L.; Chandrasekhar, J.; Madura, J. D.; Impey, R. W.; Klein, M. L. *J. Comput. Phys.* **1983**, *79*, 926.
(41) Darden, T.; York, D.; Pedersen, L. *J. Chem. Phys.* **1993**, *98*, 10089.
(42) Verlet, L. *Phys. Rev.* **1967**, *159*, 98.
(43) Berendsen, H. J. C.; Postma, J. P. M.; van Gunsteren, W. F.; DiNola, A.; Haak, J. R. *J. Comput. Phys.* **1984**, *81*, 3684.
(44) Connolly, M. L. *J. Appl. Crystallogr.* **1983**, *16*, 548.
(45) Connolly, M. L. *Science* **1983**, *221*, 709.
(46) Connolly, M. L. *J. Am. Chem. Soc.* **1985**, *107*, 1118.
(47) Sanner, M. F.; Olson, A. J.; Spehner, J. C. *Biopolymers* **1996**, *38*, 305.
(48) Richards, F. M. *Annu. Rev. Biophys.* **1977**, *6*, 151.
(49) Mandelbrot, B. B. *The Fractal Geometry of Nature*; Freeman: San Francisco, CA, 1983.
(50) Blasizza, E.; Fermeglia, M.; Pricl, S. *Mol. Simul.* **2000**, *24*, 167.
(51) Birdi, K. S. *Fractals in chemistry, geochemistry and biophysics*; Plenum Publishing Corporation: New York, 1993.
(52) Cook, G. M. W. *Biol. Rev.* **1968**, *43*, 363.
(53) Weiss, L. *Int. Rev. Cytol.* **1969**, *26*, 63.
(54) Nagy, Z.; Peters, H.; Hüttner, I. *Lab. Invest.* **1983**, *49*, 662.
(55) Pricl, S.; Fermeglia, M. *Carbohydr. Polym.* **2001**, *45*, 23.

BM049858X